



Research articles

Accounting for dynamic losses in the Jiles-Atherton model of magnetic hysteresis



Irina Podbereznyaya, Alexander Pavlenko*

Platov South-Russian State Polytechnic University (Novocherkassk Polytechnic Institute), Rostov Region, Novocherkassk, Prosveshcheniya st., 132, 346428, Russian Federation

ARTICLE INFO

Keywords:

Magnetic hysteresis
Semiconductor pulse converters
Numerical simulation
Dynamic losses

ABSTRACT

When designing semiconductor pulse converters of power systems operating in peak load conditions, it is necessary to calculate their characteristics and parameters, taking into account the magnetization reversal processes in the magnetic circuits of transformers and chokes. Magnetic materials of magnetic cores exhibit non-linear, hysteretic, and dynamic properties due to the presence of classical vortex and additional losses. Various dynamic models, based on the classical Jiles–Atherton (JA) approach, are presented in the literature, however, they are unstable for textured materials and cannot be explained from a physical point of view. These models show certain non-physical situations expressed by the deformation of the hysteresis loop in the saturation region. In this paper, the direct and inverse dynamic hysteresis models are presented, based on the application of the theory of field separation. This approach explains some of the energy aspects of the JA model.

1. Introduction^{config:prinstream}

The reliability of the calculation methods in the design of electrical devices is largely determined by the accuracy of modelling electromagnetic processes in a ferromagnet and depends on the accuracy of the presentation of the main magnetic characteristics of the magnetic circuits' materials. These characteristics determine hysteretic, vortex, and abnormal losses in the conductive structures of magnetic cores and condition their dynamic properties [1]. Of particular interest is the simulation of the hysteresis in magnetic cores of pulse transformers made of ferrite. In accordance with this, the simulation of dynamic hysteresis is a necessary condition for the accounting of the main losses. Among the existing hysteresis models, the Jiles–Atherton (JA) [2] model is most widely used because of the simplicity of the numerical simulation [3]. The model was repeatedly improved, and the anisotropy and the frequency dependence [4–7] were added to it. The inclusion schemes for the dynamic loss accounting module in the original JA model are given in [6,7]. The inverse dynamic JA models based on the principle of energy balance are presented in [8,9]. Both models give different expressions of the dynamic component of the JA model; they exhibit a deformation of the hysteresis loop in the saturation region depending on the field frequency, which is inexplicable from a physical point of view, as mentioned in [10]. According to the classical theory of electrical losses, thermal power is released in a ferromagnetic body placed

in an alternating electromagnetic field. This power, known as steel loss, is mainly the result of two physical effects. Firstly, by the effect of ohmic losses from eddy currents induced by an alternating field (losses due to eddy currents), and secondly, by the effect of cyclic magnetization reversal of magnetic material with the release of heat losses proportional to the area of the hysteresis loop (hysteresis loss). Bertotti's theory includes, in addition to losses from hysteresis and eddy currents, additional losses, called incremental losses, which for various grades of electrical steel range from 10% to 50% of the total losses [1]. It is believed that the incremental loss in steel refers to the increased losses due to eddy currents, which are obtained due to the uneven magnetization of the steel. However, neither eddy current losses nor additional losses depend on the magnetic properties of the material, which means that taking into account dynamic losses, the hysteresis loops will only expand horizontally and not stretch, as is observed in the original JA models presented in [6–9], the dynamic implementation loops of which are shown in Fig. 1. Here, curve 1 corresponds to a frequency of 50 Hz and does not take into account dynamic losses. Curves 2,3, and 4 account for dynamic losses for frequencies of 50 Hz, 100 Hz, and 150 Hz, respectively.

In this paper, we are exploring the dynamic loss accounting technique based on the theory of field separation [1,11]. The proposed model follows the physics of the process and provides a better loop shape. Model parameters were obtained from experimental curves

* Corresponding author at: Rostov Region, Novocherkassk, Prosveshcheniya st., 132, 346428, Russian Federation.

E-mail addresses: podbereznyayaib@mail.ru (I. Podbereznyaya), a.pavlenko@npi-tu.ru (A. Pavlenko).

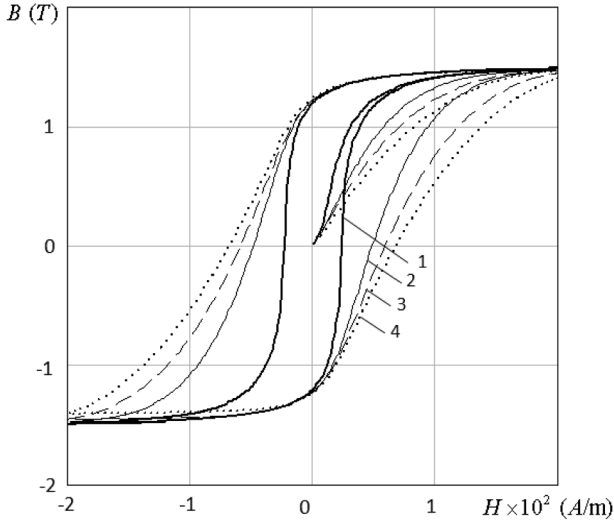


Fig. 1. The dynamic hysteresis loops based on the original JA model.

using the parameter identification method, as described in [12,13]. Experimental hysteresis curves were obtained by using the MK-3E magnetometer for steel samples (<http://www.introtest.com/index.php?page=products&pid=506>). The principle of operation of the magnetometer is to magnetize a steel sample along the main magnetization curve in a given mode and then magnetize through a hysteresis loop. Calculation of the magnetic characteristics of the test sample is based on measuring the values of magnetic induction at the points of the hysteresis loop and the main magnetization curve according to the characteristics of the magnetizing field.

In [12], a detailed two-stage technique for obtaining optimal parameters of a hysteresis model is presented, based on a real coded genetic algorithm. The first stage includes a preliminary assessment of the model parameters and their range of change. The second stage involves the implementation of a genetic algorithm. A technique with preliminary estimation of parameters and further application of the genetic algorithm allows us to obtain results with acceptable accuracy. The simulation results are confirmed by experimental studies.

2. Methods of calculating losses

The calculation of the power corresponding to the magnetic losses in steel is carried out in accordance with the following expressions for magnetic losses due to hysteresis and losses due to eddy currents:

$$P_{hyst} = k_{hyst} \cdot f \cdot B_{max}^\eta$$

$$P_{ec} = k_{ec} \cdot f^2 \cdot B_{max}^2$$

Here η the Steinmetz coefficient (1.6–2); f – frequency; B_{max}^η – the maximum value of the flux density of the magnetic field (magnetic induction), k_{hyst} , k_{ec} are the corresponding coefficients.

General magnetic losses in the form proposed by Bertotti are divided into three categories: losses due to hysteresis (P_{hyst}), proportional to the frequency f , which are the most significant components of magnetic losses at a low frequency; eddy current losses (P_{clas}) proportional to the square of the frequency; additional (abnormal) losses (P_{exc}) are proportional $f^{3/2}$. In accordance with Bertotti's theory, the expression for magnetic losses can be written in the following form [1]:

$$P(t) = P_{hyst}(t) + P_{clas}(t) + P_{exc}(t) \quad (1)$$

For low frequencies and / or thin plates, the magnetic field of the intensity $H(t)$ and induction $B(t)$ can be considered to be uniformly distributed over the cross section of the charge. Under these conditions, the separation of losses (1) corresponds to the separation of the fields [10,11,15]:

$$H(t) = H_{hyst}(t) + H_{clas}(t) + H_{exc}(t) \quad (2)$$

Here the hysteresis field $H_{hyst}(t)$ is calculated using a static hysteresis model. Classical losses $H_{clas}(t)$ depend on the specific resistance of the material ρ , the thickness of the sheet d , and the coefficient β (for a sheet of lined steel $\beta = 6$, for a cylinder $\beta = 16$, for a sphere $\beta = 20$) and are described by the formula [1]:

$$H_{clas}(t) = \frac{d^2}{2\beta\rho} \frac{dB}{dt} \quad (3)$$

The field of additional losses $H_{exc}(t)$ can be represented similarly [1,14]:

$$H_{exc}(t) = \left(\frac{GdwH_0}{\rho} \right)^{\frac{1}{2}} \left| \frac{dB}{dt} \right|^{-\frac{1}{2}} \frac{dB}{dt} \quad (4)$$

Here G is the dimensionless extinction coefficient of eddy currents ($G = 0.1356$), w the thickness of the lined steel package, sheet (plate); H_0 – a constant field taking into account the grain size.

The field separation approach can be used to extend a static JA model to a dynamic one. The static hysteresis field for the JA model $H_{hyst}(t)$ can be determined using this approach due to the energy equivalence between the energy function $P_{JA} = \oint M_{hyst} dB_e$ and the classical function $P_{JA} = \oint H_{hyst} dB$ [15,14]. Two opposing fields corresponding to the classical vortex loss field $H_{clas}(t)$ and the anomalous loss field $H_{exc}(t)$ can be included in the expression for calculating the effective field $H_e(t)$, as was proposed in [16]:

$$H_e(t) = H(t) + \alpha M(t) - (H_{clas}(t) + H_{exc}(t)) \quad (5)$$

3. Algorithms of forward and reverse dynamic models JA

The original (classical) JA model contains five parameters M_S – saturation magnetization, A/m; A – the shape parameter of the hysteresis-free magnetization curve, A/m; c – a constant of elastic displacement of domain boundaries; K – constant mobility of domains, A/m; α – magnetic coupling coefficient of domains; μ_0 – magnetic permeability of a vacuum.

3.1. The direct model

The algorithm for calculating the dynamic hysteresis loop from the direct JA model based on field separation is described in the following steps. At the time interval t , we set $B(t)$, $H_e(t - \Delta t) = 0$, $k_e = \frac{d^2}{2\beta\rho}$, $t_0 = 0$ and Δt . Then, according to the formulas in the cycle from $count=1$ to N ($N \geq 2f$ is the number of calculation points per period, which should be at least twice the frequency): we calculate the time $t = t_0 + \Delta t \cdot (count - 1)$, magnetic field strength $H(t)$ and for the next time interval we calculate $H(t + \Delta t)$. For a given time t : $\Delta H = H(t + \Delta t) - H(t)$, $M(t) = \frac{B(t)}{\mu_0} - H(t)$, $k_{exc} = k_1 \cdot (1 + k_2 B(t)^2)$ in accordance with [10]. In this case, the constant k_1 controls the area of the dynamic loops, k_2 adjusts the shape of the loop, slightly reducing its width. Next, the effective field is calculated in accordance with (5).

$$\text{Moreover, if } \frac{\Delta B}{\Delta t} \neq 0, \text{ then } H_e(t) = [H(t) + \alpha M(t)] - \left[k_e \frac{\Delta B}{\Delta t} + k_{exc} \left| \frac{\Delta B}{\Delta t} \right|^{-\frac{1}{2}} \frac{\Delta B}{\Delta t} \right] \text{ otherwise } H_e(t) = [H(t) + \alpha M(t)].$$

$$\text{Then } \Delta H_e = H_e(t) - H_e(t - \Delta t), \quad M_{an} = M_S \left[\text{cth} \left(\frac{H_e(t)}{A} \right) - \frac{A}{H_e(t)} \right], \quad \frac{dM_{an}}{dH_e} = \frac{M_S}{A} \left[1 - \text{cth}^2 \frac{H_e(t)}{A} + \left(\frac{A}{H_e(t)} \right)^2 \right], \quad \chi_f = \frac{1}{K} [M_{an} - M_1].$$

$$\text{If } (\chi_f \cdot \Delta H_e) > 0, \text{ then } \frac{dM}{dH} = \frac{\frac{\chi_f}{|\chi_f|} \chi_f + c \frac{dM_{an}}{dH_e}}{1 - \alpha \left(\frac{\chi_f}{|\chi_f|} \chi_f - c \frac{dM_{an}}{dH_e} \right)}, \text{ otherwise}$$

$$\frac{dM}{dH} = \frac{c \frac{dM_{an}}{dH_e}}{1 - \alpha \frac{dM_{an}}{dH_e}}.$$

Then we calculate $M(t + \Delta t) = M(t) + \frac{dM}{dH} \Delta H$ and

$B(t + \Delta t) = \mu_0 \cdot [H(t + \Delta t) + M(t + \Delta t)]$, $\frac{\Delta B}{\Delta t} = \frac{B(t + \Delta t) - B(t)}{\Delta t}$. We redefine the variables $B(t) = B(t + \Delta t)$, $M(t) = M(t + \Delta t)$, $He(t) = H(t + \Delta t)$ in the cycle, and continue the calculations until the end of the cycle, this time for a new countdown.

3.2. The inverse model

The inverse model algorithm is constructed in a similar way [17]. At the time interval t , we set $H(t)$, $He(t - \Delta t) = 0$, $k_e = \frac{d^2}{2\beta\rho}$, $t_0 = 0$ and Δt . We calculate the time $t = t_0 + \Delta t \cdot (\text{count} - 1)$, the magnetic field induction $B(t)$, for the next time step $(t + \Delta t)$ we calculate $B(t + \Delta t)$, for a given time: $\Delta B = B(t + \Delta t) - B(t)$, $M(t) = \frac{B(t)}{\mu_0} - H(t)$, $k_{exc} = k_1 \cdot (1 + k_2 B(t)^2)$ in accordance with [10], $\frac{\Delta B}{\Delta t} = \frac{B(t + \Delta t) - B(t)}{\Delta t}$. Next, we calculate the effective field, as in the previous version for the direct model: $He(t)$, ΔHe , M_{an} , $\frac{dM_{an}}{dHe}$, χ_f . If $(\chi_f \cdot \Delta He) > 0$, then $\frac{dM}{dB} = \frac{1}{\mu_0} \left(\frac{\chi_f}{|\chi_f|} \chi_f + c \frac{dM_{an}}{dHe} \right)$, otherwise $\frac{dM}{dB} = \frac{1}{\mu_0} \left(c \frac{dM_{an}}{dHe} \right)$. Then we calculate $M(t + \Delta t) = M(t) + \frac{dM}{dB} \Delta B$ and $H(t + \Delta t) = \left[\frac{B(t + \Delta t)}{\mu_0} - M(t + \Delta t) \right]$. We redefine the variables $H(t) = H(t + \Delta t)$, $M(t) = M(t + \Delta t)$, $He(t) = H(t + \Delta t)$ and continue to do so till the end of cycle.

It should be noted that the direct JA model is used in modeling processes in electromagnetic devices controlled by current sources. If the devices are controlled by a voltage source, then the inverse JA model is used.

4. Numerical modeling

Figs. 2–6 present the results of modeling dynamic hysteresis loops based on the application of the classical JA model and the field separation model. When determining the parameters of the models, the experimental data of hysteresis curves were used for isotropic electrical steel and transformer steel (anisotropic material) [25]. In Figs. 2, 4, 6 points indicate the experimental data; solid curves show the simulation results.

Design loops with parameters $M_S = 1580000$, A/m; $A = 105$, A/m; $c = 0.27$; $K = 57.3$, A/m; $\alpha = 0.0002$: excluding dynamic losses 1 – for a frequency of 50 Hz; taking into account dynamic losses for frequencies: 2–50 Hz, 3–100 Hz, 4–150 Hz. The dependencies of the induction and

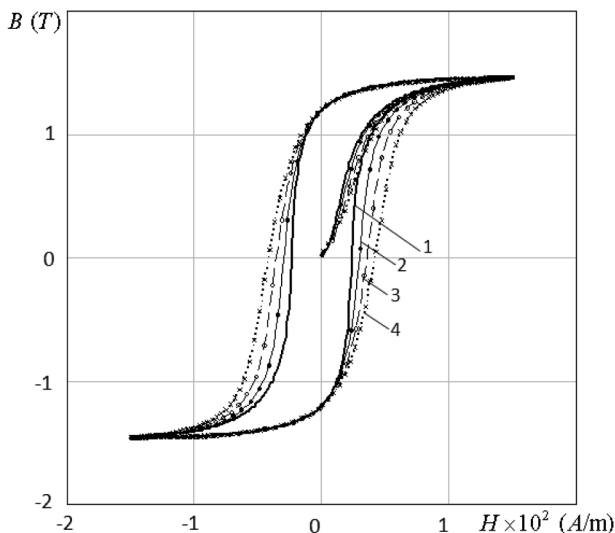


Fig. 2. Dynamic hysteresis loops obtained by the direct JA model based on field separation for steel M330-35A(RD).

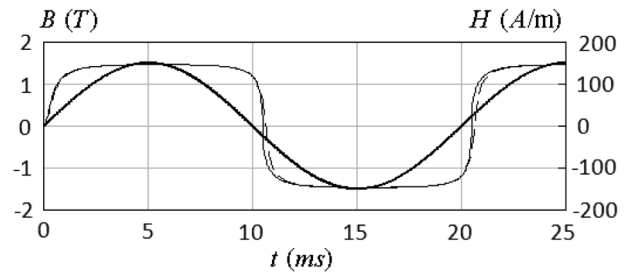


Fig. 3. Dependences of induction on the magnetic field calculated by the direct JA model based on field separation.

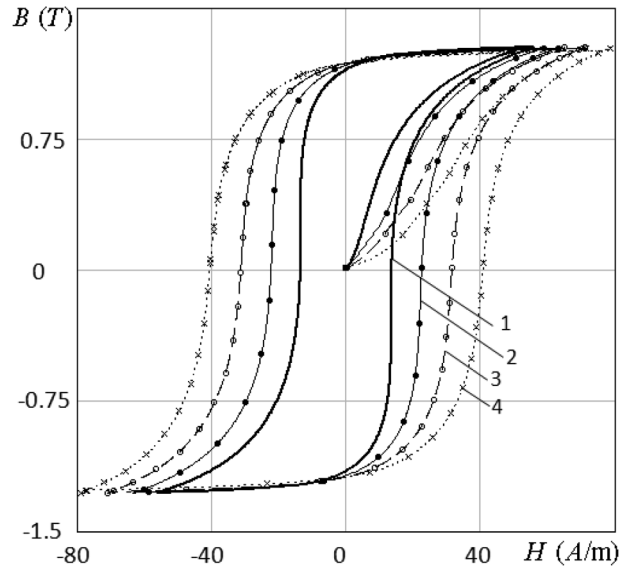


Fig. 4. Dynamic hysteresis loops obtained by the inverse JA model based on field separation for isotropic steel.

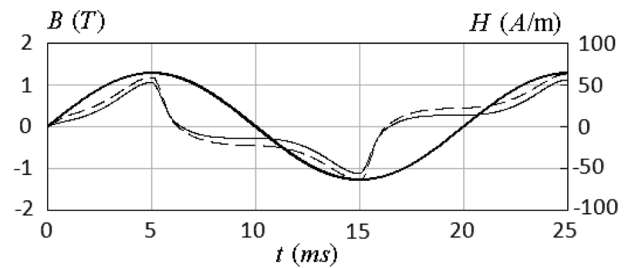


Fig. 5. Dependences of the magnetic field on induction calculated by the inverse JA model based on field separation.

magnetic field strength, unfolded over time, are shown in Fig. 3. The sinusoidal curve of the direct model JA corresponds to the magnetic field strength. On the graph, a solid thin line corresponds to induction for a variant without taking into account dynamic losses for a frequency of 50 Hz, a thin dashed line for a variant taking into account dynamic losses for a frequency of 50 Hz. Fig. 4 shows the dynamic hysteresis loops calculated using the inverse JA model. The model parameters are: $M_S = 1243100$, A/m; $A = 10$, A/m; $c = 0.27$; $K = 23.5$, A/m; $\alpha = 0.00032$: curve 1, for a frequency of 50 Hz – excluding dynamic losses; curve 2 – taking into account dynamic losses for a frequency of 50 Hz, 3–100 Hz, 4–150 Hz.

Dependencies of the magnetic field on the induction, time-developed, calculated by the inverse model JA, are shown in Fig. 5. Here, a sinusoidal curve corresponds to the induction of the magnetic field. The solid thin line corresponds to the magnetic field strength for a

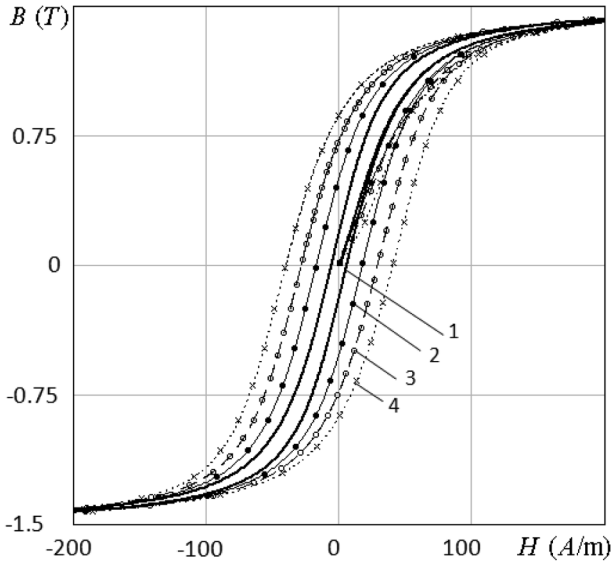


Fig. 6. Dynamic hysteresis loops obtained by the inverse JA model based on field separation for anisotropic steel M130-27s.

frequency of 50 Hz without taking into account dynamic losses, and the thin dashed line corresponds to the strength taking into account dynamic losses. The dynamic hysteresis loops obtained by the inverse JA model for anisotropic steel M130-27 s are shown in Fig. 6. The model parameters are: $M_S = 1220000$, A/m; $A = 15.1$, A/m; $c = 0.59$; $K = 15.1$, A/m; $\alpha = 1.66 \cdot 10^{-6}$. Curve 1 corresponds to the option without taking into account dynamic losses for a frequency of 50 Hz; 2 – taking into account dynamic losses for frequencies – 50 Hz, 3–100 Hz, 4–150 Hz.

Simulation errors slightly increase with increasing frequency, but do not exceed 2%. Such a good match was achieved thanks to the field separation method [1,10,21,23] and the application of the algorithm proposed in [16]. The slight increase in simulation error (up to 2%) with increasing frequency can be explained by the small drift of the parameters of the static JA model depending on the frequency. It should be noted that the JA model is a simulation model and has no physical basis. A feature of modeling grain-oriented electrical steels should be noted. Granular oriented (GO) materials are often used in electromagnetic instrument systems due to their good magnetic properties in the rolling direction (RD). These materials provide low loss and high permeability in RD due to their magneto-crystalline textured structure (Goss structure). It plays an important role in the process of magnetization of the layer [18]. As a result of this, the hysteretic characteristics of GO materials have a very steep rise and a sharp descent resembling a gooseneck [10,5], in addition, these materials have a complex characteristic in the transverse direction of rolling (TD). This, in turn, prohibits us to accurately describe the magnetization reversal processes using the classical JA model. This is mainly associated with setting a hysteresis-free magnetization curve using the Langevin function [19]. In [20], the modified JA model is based on replacing the Langevin function with the Brillouin function [19]. This significantly improves the presentation of the hysteresis loop in the RD direction, but does not allow one to correctly judge the hysteresis in other directions. In [23], it was proposed that the hysteresis-free magnetization be taken into account through additional (anisotropic) energy, since the contribution of the rotation of the domain magnetization to the magnetization process occurs through the anisotropy energy. This approach allows one to approximate the asymmetry of the slopes of the lower and upper branches of the loop. As a result, hysteresis-free magnetization can be expressed as a function [24]:

$$M_{an} = M_S \frac{\int_0^\pi e^{\frac{E(1)+E(2)}{2}} \sin \theta \cos \theta d\theta}{\int_0^\pi e^{\frac{E(1)+E(2)}{2}} \sin \theta d\theta} \quad (6)$$

where uniaxial anisotropy ($i = 1, 2$) is determined in accordance with [24]:

$$E(i) = \left(\frac{He(t)}{A} \right) \cos \theta - \frac{K_{an}}{M_S \mu_0 A} \sin^2(\phi_i)$$

For GO steel, this expression can be represented as [22]:

$$E(i) = \left(\frac{He(t)}{A} \right) \cos \theta - \frac{K_{an}}{M_S \mu_0 A} \times \left(\cos^2(\phi_i) \sin^2(\phi_i) + \frac{\sin^4(\phi_i)}{4} \right)$$

where K_{an} is the average energy density of anisotropy, which is an analog of the magnetic anisotropy coefficient in accordance with the Bloch domain wall model, $\phi_1 = (\psi - \theta)$ and $\phi_2 = (\psi + \theta)$, where ψ is the angle between the direction of magnetization and the axis of easy magnetization of the material. For an isotropic material (where $K_{an} = 0$), the equation reduces to the Langevin function:

$$M_{an} = M_S \left[\operatorname{cth} \left(\frac{He(t)}{A} \right) - \frac{A}{He(t)} \right]$$

Equation hysteresis-free magnetization (6) can be solved using standard methods of numerical integration. The JA model now requires knowledge of another sixth parameter K_{an} . If we make the appropriate replacements, we get a model that accurately describes the processes in grain-oriented ferromagnets (Fig. 6). It should be noted that the magnetic characteristics of GO-steels are specific. The classical approach of taking into account dynamic losses in the static JA model leads to an insignificant expansion of the hysteresis loop and to its horizontal stretching, which does not correspond to real physical processes. The hysteresis loops should only expand horizontally, and not stretch, since the additional losses do not depend on the magnetic properties of the material. In the second case, the inclusion of dynamic losses in the static JA model is based on the principle of field separation (equations (1)-(4)). This gives better results and converts the hysteresis loop by expanding rather than stretching. Sometimes applying the principle of separation of fields is not enough. In this case, other methods considered in Section 4 can be used. In the present work, we managed to implement this on the basis of the principle of field separation.

Dynamic hysteresis loops for ferrite grade MBW093, at different frequencies are shown in Fig. 7. The model parameters are: saturation induction – $B_s = 0.47$ T; residual induction – $B_r = 0.167$ T; induction coercive force – $H_{cB} = 21$ A/m; saturation magnetic field strength – $H_S = 1200$ A/m; saturation magnetization – $M_S = 373003.8217$ A/m; shape parameter of a hysteresis-free magnetization curve – $A = 35$ A/m; constant domain mobility – $K = 40$ A/m; constant of elastic displacement of domain boundaries – $c = 0.000001$, magnetic coupling coefficient of domains – $\alpha = 0.00012$. In Fig. 7 lines represent the simulation results, dots – experimental curves: 1 – $f = 50$ Hz, 2 – $f = 1000$ Hz, 3 – $f = 5000$ Hz, 4 – $f = 10000$ Hz.

5. Conclusion

In this paper, we present two modified Jiles-Atherton dynamic models (forward and reverse) for calculating the magnetization curves and magnetic power losses in charge steel and use them as component models in the analysis of processes in semiconductor converters. Both models are derived from field separation theory. Numerical studies

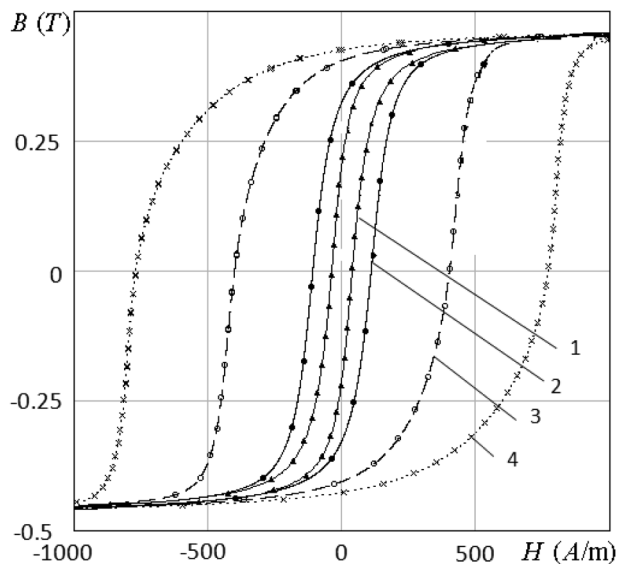


Fig. 7. Hysteresis loops for the MBW093 ferrite.

show that the models accurately reproduce real hysteresis dependences for different ferromagnetic materials. It was found that the errors in the simulation increase with increasing frequency, but do not exceed 2%. It should be noted that all modifications of the Jiles-Atherton model require additional verification and proper parameter settings in connection with various properties of magnetic materials.

CRediT authorship contribution statement

I.B. Podbereznyaya: Conceptualization, Data curation, Formal analysis, Funding acquisition. **A.V. Pavlenko:** Investigation, Methodology, Project administration, Resources, Supervision, Validation.

Declaration of Competing Interest

The authors declare that they have no known competing financial interests or personal relationships that could have appeared to influence the work reported in this paper.

Acknowledgments

This article was prepared based on the results obtained during the implementation of the state task to carry out fundamental research (project “Hydrogen fuel cell energy units for small unmanned aerial vehicles: modeling, development, research”, the customer is the

Ministry of Science and Higher Education of the Russian Federation, scientific theme code is FENN-2020-0020).

References

- [1] G. Bertotti, *Hysteresis in Magnetism*, Academic, San Diego, CA, USA, 1998.
- [2] D.C. Jiles, D.L. Atherton, Theory of ferromagnetic hysteresis, *J. Magn. Magn. Mater.* 61 (1–2) (1986) 48–60.
- [3] H.L. Toms, R.G. Colclaser, M.P. Krefta, Two-dimensional finite element magnetic modeling for scalar hysteresis effects, *IEEE Trans. Magn.* 37 (2) (2001) 982–988.
- [4] D.C. Jiles, A self consistent generalized model for the calculation of minor loops excursions in the theory of hysteresis, *IEEE Trans. Magn.* 28 (5) (1992) 2602–2604.
- [5] A.P.S. Baghel, S.V. Kulkarni, Hysteresis modeling of the grainoriented laminations with inclusion of crystalline and textured structure in a modified Jiles-Atherton model, *J. Appl. Phys.* 113 (4) (2013) pp. 043908-1–043908-5.
- [6] D.C. Jiles, *IEEE Trans. Magn.* 30 (1994) 4326.
- [7] D.C. Jiles, Frequency dependence of hysteresis curves in conducting magnetic materials, *J. Appl. Phys.* 76 (10) (1994) 5849–5855.
- [8] K. Chwastek, Modeling of dynamic hysteresis loops using the Jiles-Atherton approach, *Math. Comput. Model. Dyn. Syst.* 15 (1) (2009) 95–105.
- [9] H. Li, Q. Li, X. Xu, T. Lu, J. Zhang, L. Li, A modified method for Jiles-Atherton hysteresis model and its application in numerical simulation of devices involving magnetic materials, *IEEE Trans. Magn.* 47 (5) (2011) 1094–1097.
- [10] S.E. Zirka, Y.I. Moroz, R.G. Harrison, K. Chwastek, On physical aspects of the Jiles-Atherton hysteresis models, *J. Appl. Phys.* 112 (4) (2012) pp. 043916-1–043916-7.
- [11] S.E. Zirka, Y.I. Moroz, P. Marketos, A.J. Moses, D.C. Jiles, T. Matsuo, Generalization of the classical method for calculating dynamic hysteresis loops in grain-oriented electrical steels, *IEEE Trans. Magn.* 44 (9) (2008) 2113–2126.
- [12] I.B. Podbereznyaya, V.V. Medvedev, A.V. Pavlenko, I.A. Bol’shenko, Selection of Optimal Parameters for the Jiles–Atherton Magnetic Hysteresis Model, *Russian Electrical Engineering.* 90 (1) (2019) 80–85.
- [13] A.P.S. Baghel, S.V. Kulkarni, Parameter identification of the Jiles-Atherton hysteresis model using a hybrid technique, *IET-Electr. Power Appl.* 6 (Nov. 2012) 689–695.
- [14] A.P.S. Baghel, S.V. Kulkarni, Dynamic loss inclusion in the Jiles–Atherton (JA) hysteresis model using the original JA approach and the field separation approach, *IEEE Trans. Magnet.* 50 (2) (2014) 369–372.
- [15] R. Venkataraman and P. Krishnaprasad, “Qualitative analysis of a bulk ferromagnetic hysteresis model”, in *Proc. 37th IEEE Conf. Decision Control*, vol. 3. Dec. 1998, pp. 2443–2448.
- [16] M. Hamimid, S.M. Mimoune, M. Feliachi, Hybrid magnetic field formulation based on the losses separation method for modified dynamic inverse Jiles-Atherton model, *Phys. B, Condensed Matter* 406 (14) (2011) 2755–2757.
- [17] N. Sadowski, N.J. Betistela, J.P.A. Bastos, L.M. Mazenc, An inverse Jiles-Atherton model to take into account hysteresis in timestepping finite-element calculations, *IEEE Trans. Magn.* 38 (2) (Mar. 2002) 797–800.
- [18] V. Paltanea, G. Paltanea, *Mater. Sci. Forum* 670 (2011) 66.
- [19] S. Chikazumi, *Physics of Ferromagnetism*, Oxford Univ. Press, New York, 1997.
- [20] K. Chwastek, J. Szczygłowski, The effect of anisotropy in the modified Jiles-Atherton model of static hysteresis, *Arch. Electr. Eng.* 60 (2011) 49.
- [21] A. Ramesh, D.C. Jiles, J.M. Roderick, *I.E.E.E. Trans. Magn.* 32 (1996) 4234.
- [22] A.P.S. Baghel, S.V. Kulkarni, *J. Appl. Phys.* 113 (2013) 043908.
- [23] A.P.S. Baghel, S.V. Kulkarni, Dynamic loss inclusion in the Jiles-Atherton (JA) hysteresis model using the original JA approach and the field separation approach, *IEEE Trans. Magn.* 50 (2) (Feb. 2014) 369–372.
- [24] R. Szweczyk, P. Cheng, Open source implementation of different variants of Jiles-Atherton model of magnetic hysteresis loops, *J. Acta Physica Polonica A* 133 (3) (Mar. 2018) 654–656.
- [25] S. Bi, Charakterisieren und modellieren der ferromagnetischen hysteresis, Ph.D. dissertation Friedrich-Alexander-Universität Erlangen-Nürnberg, 2014.